Qualification Flight Tests of the Viking Decelerator System

R. D. MOOG*
Martin Marietta Corporation, Denver, Colo.
AND
R. J. BENDURA† AND J. D. TIMMONS‡
NASA Langley Research Center, Hampton, Va.
AND
R. A. LAU§
Goodyear Aerospace Corporation, Akron, Ohio

The Balloon Launched Decelerator Test (BLDT) series conducted at White Sands Missile Range (WSMR) during July and August of 1972 flight qualified the NASA Viking '75 decelerator system at conditions bracketing those expected for Mars. This paper discusses the decelerator system design requirements, compares the test results with prior work, and discusses significant considerations leading to successful qualification in Earth's atmosphere. The Viking decelerator system consists of a single-stage mortar-deployed 53-ft nominal dia. disk-gap-band parachute. Full-scale parachutes were deployed behind a full-scale simulated Viking vehicle at Mach numbers from 0.47 to 2.18 and dynamic pressures from 6.9 to 14.6 psf. Analyses show that the system is qualified with sufficient margin to perform successfully for the Viking mission. The canopy maintains a stable drag shape after initial inflation oscillations and was not affected by aeroshell separation. The parachutes exhibited canopy fluctuations as predicted above subsonic velocities. Parachute transonic drag was degraded by the forebody wake verifying wind-tunnel test results. Analyses show maximum suspended vehicle attitude rates near 100° per second on Mars due to opening shock. During terminal descent, attitude rates damp to less than 30° per second.

Introduction

THE Viking '75 mission will soft land two scientific packages on the surface of Mars. Even with the advent of Mariner 9 which has contributed much to our knowledge of Mars, there still exist large uncertainties about the Martian atmospheric densities and scale heights. These uncertainties manifest themselves in divergent design requirements for any aerodynamic decelerator to be employed. For example, the Viking disk-gap-band (DGB) parachute must be designed to be functional at Mach numbers from 2.0 to low subsonic and perform without damage in a range of dynamic pressures from 10 psf to 0.5 psf. In addition, stringent Viking mission requirements impose the constraints of minimum decelerator system weight and volume, maximum and minimum allowable drag, minimum deployment loads, and no particulate contamination.

A special concern is that the parachute must function with adequate performance and without damage in the turbulent wake of a large blunt lifting entry vehicle for an extended period of time. Wind-tunnel development tests of scale-model parachutes indicated that the entry vehicle wake adversely affects parachute performance under certain conditions.[1] The results of these tests were utilized to design a system exhibiting minimum performance degradation in the wind tunnel.

During the decelerator development phase, parachute design and functional sequencing were explored and verified by means of wind-tunnel testing and low-altitude drop tests.[2] Both of these methods have deficiencies, therefore a free-flight program was utilized to qualify a full-scale Viking decelerator system and full-scale blunt forebody at Earth altitudes which would more accurately simulate parachute deployment conditions on Mars.

The qualification program consisted of a series of four Balloon Launched Decelerator Tests (BLDT) covering three different Mach number regimes and encompassing the entire range of significant parachute conditions for the postulated Martian atmosphere models. The major program objectives were to evaluate system performance in the wake of a large forebody in a wide Mach number regime, verify structural integrity of the system, and determine decelerator system and separating aeroshell effects on the entry vehicle.

The tests were conducted over the White Sands Missile Range during July and August 1972. Test data for each flight are presented in Ref. 3–6. The purpose of this paper is to review pertinent decelerator system design requirements, to discuss results of analysis based on data from all BLDT flights and, in some cases, compare these results with both theory and other flight data.

Viking Decelerator System

The Viking decelerator system includes a 53-ft nominal diam (D_o) disk-gap-band (DGB) parachute with $1.70D_o$ suspension lines, a swivel located at the confluence point, three 7.5-ft bridle legs, and a mortar for deployment.

Viking mission constraints require the system to be biologically clean and not produce particulate debris which resulted in: 1) the use of scoured Dacron 52 cloth and tapes in order to eliminate all oils and cloth "sizing," 2) retention of all parts, and 3) the system to undergo a heat sterilization environment of 280°F for 200 hr. These, in turn, presented the problems (successfully solved) of designing a minimum weight system which would neither shrink nor degrade in strength after exposure to high heat and in the absence of all lubricants and water. Additionally, the system must perform after being packed at a density of about 40 lb/ft^3 and stored in this condition for about 34 months.

Presented as Paper 73-457 at the AIAA Fourth Aerodynamic Deceleration Systems Conference, Palm Springs, Calif., May 21–23, 1973; submitted July 16, 1973; revision received November 12, 1973.

Index category: Entry Deceleration Systems and Flight Mechanics (e.g., Parachutes).

* Staff Engineer. Member AIAA.
† Aerospace Technologist. Member AIAA.
‡ Technical Engineer.
§ Systems Analysis Engineer.

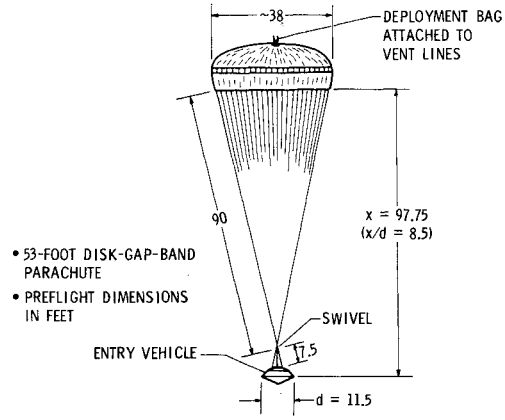

Fig. 1 Viking decelerator system. All dimensions in feet.

Parachute

Figure 1 shows the general preflight parachute/test vehicle relationship. Parachute geometric properties are shown on Table 1. The disk cloth is 2.25 oz/yd^2 rip stop material and the band is 1.53 oz/yd^2 rip stop material. The minimum strengths of the radial tapes, circumferential tapes, gap tapes, and suspension lines are 900 lb, 1800 lb, 900 lb, and 880 lb, respectively. Each bridle leg is fabricated of four plies of DuPont special fiber webbing having a break strength of 13,500 lb per ply. The swivel is designed for a minimum strength of 26,650 lb with a 1.5 safety factor.

Mortar

A single-stage mortar is used to eject the packed parachute from the rear of the spacecraft. The mortar has a volume of 2.2 ft^3 and is designed to eject a total mass of about 102 lb at velocities near 112 fps at test altitude. Ejected components for the BLDT flights weighed 97 lb and included parachute assembly, deployment bag, cover, and sabot. The mortar breech contains an erodible orifice designed to maintain constant pressure in the mortar tube during ejection. Further information about the mortar may be found in Refs. 7 and 8.

Test System

Four tests were conducted, two at supersonic conditions and one each at transonic and subsonic conditions. The target test conditions were Mach number and dynamic pressure which occur at Earth altitudes near 140,000 ft for all but the subsonic test. A combination of balloons and rockets, similar to that utilized for the PEPP tests,[9] were employed to reach the desired test altitude. The typical flight sequence for the powered flights is shown in Fig. 2. The subsonic test did not need propulsion units, but involved simply a free-fall drop from the balloon to a test altitude near 87,000 ft.

Table 1 Parachute geometric properties (preflight)

Item	Relative value	Value
Nominal diameter	D_o	53 ft
Geometric porosity[a]	0.125 S_o	276 ft^2
Total area (S_o)[b]	$(\pi/4)\ D_o^2$	2206.2 ft^2
Disk area[c]	0.53 S_o	1169.3 ft^2
Disk diameter	0.726 D_o	38.5 ft
Disk circumference	2.285 D_o	121 ft
Gap area	0.12 S_o	264.7 ft^2
Gap width	0.042 D_o	2.2 ft
Band area	0.35 S_o	772.2 ft^2
Band width	0.121 D_o	6.4 ft
Vent area	0.005 S_o	11.0 ft^2
Vent diameter	0.07 D_o	3.7 ft
Number of suspension lines	—	48
Length of suspension lines	1.7 D_o	90 ft

[a] Vent plus gap provide 12.5% geometric porosity.
[b] Disk + gap + band.
[c] Includes vent.

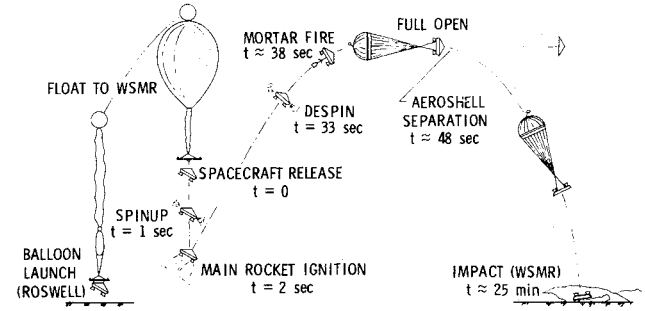

Fig. 2 Typical mission sequence—powered flight.

The test vehicle (Fig. 3) was physically similar to the Viking entry vehicle except for the protruding rocket motor nozzles required on the powered vehicles. The test vehicle weighed approximately 1890 lb at decelerator deployment on each of the flights. Onboard instrumentation included forward and aft-looking cameras, bridle leg tensiometers, rate gyros, and accelerometers. More detailed information on the test system, test system performance, and test operations is included in Refs. 3–6 and 10.

Mars Qualification

To qualify a parachute system for utilization on Mars, it is necessary to bracket the range of dynamic pressures and Mach numbers predicted for Mars flight. The Mars envelope of these parameters and the actual BLDT test points (to be discussed) are shown in Fig. 4. Specific test objectives for each test flight (designated by AV number) were as follows: AV-1) Demonstrate performance and structural integrity at deployment conditions in excess of maximum Mars dynamic pressure and in excess of Mach 2.0. AV-2) Demonstrate performance at deployment conditions in the transonic region and at a dynamic pressure lower than the lowest expected for Mars. AV-3) Demonstrate performance at deployment conditions at a velocity less than expected for Mars. AV-4) Reflight of AV-1 but targeted to reflect changes resulting from Mariner 9 data.

General Parachute System Performance Objectives

Additional general qualification objectives for all BLDT flights are: 1) Verify that the mortar provides a minimum of 94 fps ejection velocity. 2) Determine line stretch, bag strip, and inflation times. 3) Photographically record the time history of

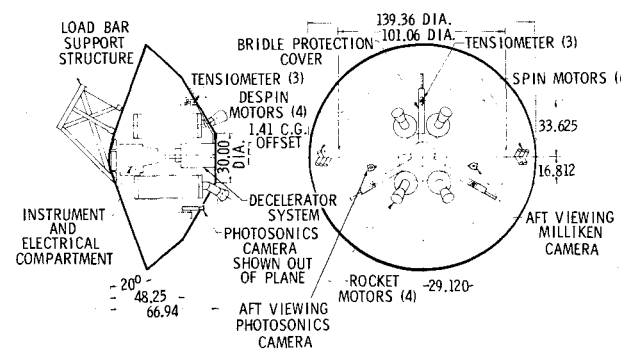

Fig. 3 BLDT supersonic vehicle. All dimensions in inches.

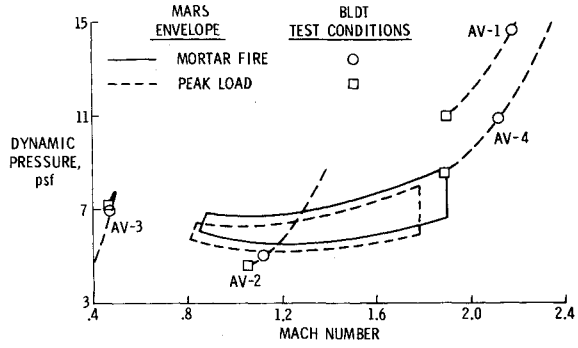

Fig. 4 Mars envelope and test conditions.

canopy stability during the inflation phase. 4) Verify that the parachute drag coefficient falls within the envelope of Fig. 14.[11] 5) Demonstrate parachute structural integrity at a load condition 30% greater than the maximum predicted peak load conditions for Mars. 6) Vehicle oscillations shall be less or equal to $\pm 25°$ amplitude in quasi-steady-state descent with no wind when analytically extrapolated to Mars conditions. 7) Vehicle attitude rates shall be less or equal to 30° per second in quasi-steady-state descent with no wind when analytically extrapolated to Mars conditions.

Loads Criteria

The critical load test for the parachute is the supersonic case and the objective for this test is to obtain peak load conditions that exceed the Mach number and dynamic pressure envelope defined in Fig. 4. In establishing these load limits, the effective design dynamic pressure for BLDT is adjusted downward to compensate for increased aerodynamic heating and load amplification effects and adjusted upward for the absence of interplanetary cruise degradation. These adjustments are made to compensate for relative changes in the parachute structural capability between BLDT and Mars as follows:

$$q[\text{BLDT}] = (W) \cdot (X) \cdot (Y) \cdot (Z) \cdot q\ [\text{Mars design limit}]$$

where: W = margin of overtest = 1.3 max.; X = aerodynamic heating factor = 0.985; Y = amplification effect = 0.95; Z = interplanetary cruise degradation = 1.03.

Parachute Deployment Conditions

Parachute deployment conditions (mortar fire) on the BLDT flights differ from the Viking conditions in several important respects. The BLDT vehicle had to accept the residual effects of a powered-flight phase which included spinup, despin, and main engine thrust tail off. Second, the BLDT vehicle, unlike the Viking entry vehicle, did not have an active attitude-control system and could not control attitude rates or angles of attack and sideslip at deployment.

The primary purpose of each BLDT vehicle was to achieve parachute deployment conditions which fell within the desired qualification envelopes discussed in Ref. 10. This was accomplished for each test condition by selecting the proper drop attitude from the balloon, choosing the number and type of rocket motors for the desired thrust, and firing the mortar either by ground command or by airborne timer. Within these design constraints, the actual deployment conditions were further influenced by numerous flight performance dispersions which were, to some degree, predictable but had to be controlled as tightly as possible.

A summary of actual parachute deployment conditions achieved on each of the BLDT flights and the launch dates is presented in Table 2.

The actual deployment conditions are compared to the qualification envelopes in Ref. 10. With the exception of AV-1 which was subsequently ruled a "no test," all flight-test peak load points fell within the desired qualification envelopes. An overview of all the test points plotted with relation to the latest Mars envelope in Fig. 4 shows that the decelerator has truly been tested at conditions (deployment and peak load) that encompass upper and lower limits of Mach number and dynamic pressure.

A review of some of the other deployment conditions from Table 2 reveals additional qualification data. The maximum BLDT total angle of attack of 13° compares favorably with the Mars nominal trim condition of 11.9° at Mach 2.0. Stowed parachute temperature conditions on all flights were lower than the 80°F requirement to limit aerodynamic heat degradation of the canopy at the higher Mach number conditions.

The attitudes and attitude rates for BLDT are indicative of vehicle dynamic motions which are significantly higher than what is expected on Mars. An indication of how far each vehicle was away from its trim condition at deployment is obtained by computing the vector difference between total angle of attack at deployment and at aerodynamic trim. This vector difference, shown as deviation from trim in Table 2 was as high as 10.4° on BLDT whereas the Viking vehicle oscillation about trim is expected to be $\pm 3°$. Attitude rates as high as 14° per second on BLDT compare with Viking rates that are controlled by an attitude-control system to approximately 1° per second.

Mortar Performance

The minimum Viking mortar muzzle velocity defined by the above conditions is 94 fps.[7] On the supersonic BLDT flight tests (AV-1 and AV-4) where a 1.3 overload in dynamic pressure is targeted, the increased BLDT deceleration adds approximately 10 fps to the mortar velocity requirement to achieve equivalence between BLDT and Viking during the bag strip process. A mortar design was chosen which had the additional margin of ejection velocity to make it suitable for both BLDT and Viking. Preliminary results from mortar development tests[7] conducted in a chamber where altitude and temperature could be simulated showed a mean mortar velocity of 110.6 fps with a standard deviation of 4.42 fps.

Actual BLDT mortar performance is evaluated by observing the bag stripping process from onboard cameras. When the suspension lines are fully payed out of the deployment bag, line stretch occurs and the canopy starts emerging from the bag. This event causes an identifiable spike to occur on the telemetered tensiometer loads and can readily be identified on the onboard film. The time from mortar fire to line stretch is therefore accurately determined. The actual distance the deployment bag must travel for the suspension lines to be pulled from the bag is defined by the length of the lines themselves. For most of the low dynamic pressure applications that are typical of the Mars deployment, the lines may be assumed to follow a straight

Table 2 BLDT parachute deployment conditions

	AV-1	AV-2	AV-3	AV-4
Mach number	2.18	1.133	0.47	2.126
Dynamic pressure, psf	14.63	5.00	6.9	10.90
Velocity, fps	2314	1194	464	2290
Axial acceleration, g's	−1.18	−0.40	−0.34	−0.93
Altitude, feet	142025	135368	87027	147186
Angle of attack, degrees	−12	5.4	3.5	−4.1
Angle of sideslip, degrees	−2	−4.9	−4.5	−3.1
Total angle of attack, degrees	13	7.28	5.7	5.2
Parachute temperature, °F	50	47	26	46
Residual spin rate, deg/sec	−26	−62	−0.5	−30
Pitch rate, deg/sec	2	13	2.1	−14
Yaw rate, deg/sec	−3	3	−5.8	4
Trim angle of attack, degrees	−8.5	−3.7	−4.3	−9
Deviation from trim, degrees	4	10.4	9.1	6
Launch date	7/11/72	7/26/72	8/19/72	8/13/72

Table 3 BLDT mortar performance

	AV-1	AV-2	AV-3	AV-4
Mortar velocity, fps	112	106.5	112	114.2
Time to line stretch, sec	1.03	1.015	0.96	0.99
Relative velocity at line stretch	72	92.6	91.8	86.4
Time to bag strip, sec	1.40	1.31	1.32	1.30
Relative velocity at bag strip	71.5	83.9	84.3	83.6

line between lander and the bag. For higher dynamic pressure and angle-of-attack conditions such as were experienced on AV-1, a line bowing correction was applied to account for the aerodynamic influence on the lines. By simulating the mortar firing process with complete aerodynamic forces and momentum exchange between the forebody and the deployment bag, a mortar velocity can be deduced. A summary of the mortar performance determined from a review of the flight data and simulation is presented in Table 3.

All the BLDT flight mortar velocities exceed the minimum Viking requirement of 94 fps and show a substantial relative velocity remaining at bag strip to assure positive bag strip. There appears to be a fair amount of variation in mortar velocity from flight to flight. A preliminary review of all the ground and flight mortar data of a common design show that the mean mortar velocity is 110.8 fps with a standard deviation of 3.8 fps. The chance of the mortar velocity being as low as 94 ft/sec is seen to be extremely remote.

Parachute Inflation Characteristics

The filling times for the BLDT flights are summarized in Table 4 and are plotted in Fig. 5 along with flight-test data from the low-altitude bomb drop development tests[2] and Planetary Entry Parachute Program (PEPP) results.[12] The data which use bag strip as a zero time reference agree reasonably well with the filling time equation taken from the parachute handbook[13] ($t_f = 0.65 \cdot \lambda_G \cdot D_o/V$). Bag strip is used here as a filling time zero reference in the classical sense, as defining a point where all the canopy cloth has been removed from the bag and is stretched

Table 4 Parachute inflation characteristics

	AV-1	AV-2	AV-3	AV-4
Filling time from line stretch, sec	0.56	0.64	0.81	0.56
Filling time from bag strip, sec	0.25	0.35	0.52	0.312
Vehicle velocity at line stretch, fps	2250	1160	459	2245
Vehicle velocity at bag strip, fps	2218	1150	458	2235

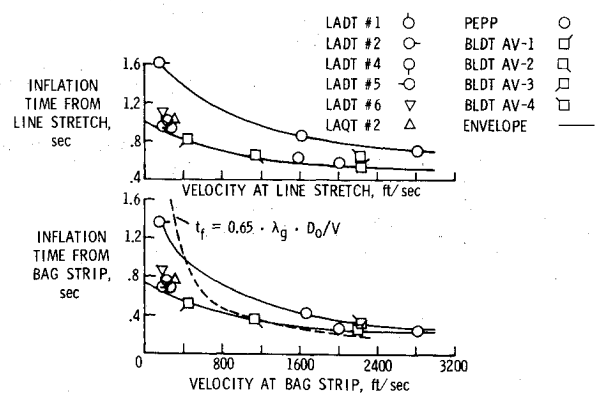

Fig. 5 Parachute filling time data.

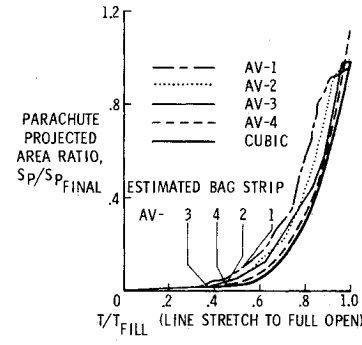

Fig. 6 Canopy growth parameter.

out but uninflated. Bag strip, however, is difficult to determine accurately from the onboard camera data because the bag disappears from view behind the inflating canopy. The data in Fig. 5 which use line stretch as a time reference are more accurate because this event can be observed as first canopy emergence from the bag on the film data and as a jump in telemetered line load. The envelope of test data thus established provides good assurance that large uncertainties in filling time are unlikely.

The growth of the canopy from line stretch was obtained by integrating the projected area images from the Milliken camera. A canopy growth parameter curve of normalized area ($S_P/S_{P\,FINAL}$) versus time for each parachute test is included in Fig. 6. The projected area at any time is divided by the projected area in the final seconds of airborne film coverage (50 sec after mortar fire). The time scale is normalized by the total filling time from line stretch. Comparison of the BLDT canopy growth curves shows them all to be well behaved and very similar. The curve for AV-1, as might be expected, showed the effect of a damaged canopy by deviating most significantly from the others. That part of the inflation curve from bag strip to full open is seen to be approximated very closely by a cubic function of time.

After first full inflation, the canopy typically goes through a short period of unstable inflation shown in Fig. 7. The BLDT canopy behavior is very similar to that shown on previous disk-gap-band tests in the PEPP series, and, like PEPP, showed increased instability at the supersonic deployment conditions. Two dips in projected area, one at 2.0 sec on AV-2 and another at 2.5 sec on AV-4 are more pronounced than previously seen on PEPP. These appear to be caused by the canopy operating in the turbulent wake of the large forebody. After the short period of area oscillations shown in Fig. 7, the canopy achieved steady inflation and remained stable thereafter. No correction has been applied to the parachute projected area ratio to account for variation in the canopy image plane under changing load conditions.

Opening Load and Prediction Methods

Opening load prediction has made rapid strides in recent years with the aid of high-speed digital computers. The work of

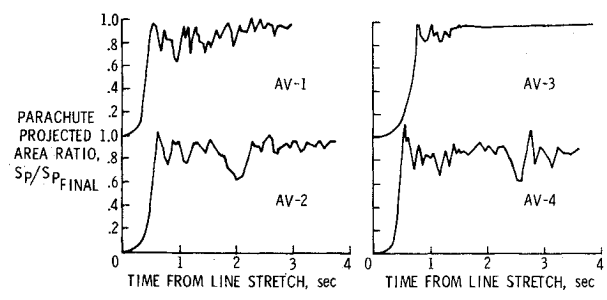

Fig. 7 Canopy area oscillations.

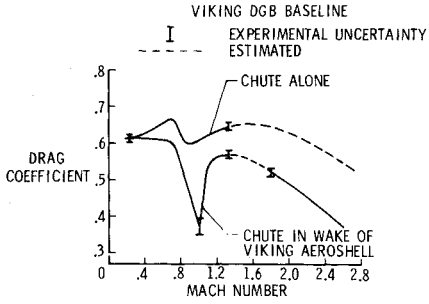

Fig. 8 Wind-tunnel drag data.

Heinrich and Noreen,[14] Berndt and DeWeese,[15] and Toni[16] have contributed notably toward an understanding of the parachute opening load problem. However, in spite of all this progress, opening load prediction is still very difficult because the nonrigid structure is made of textiles with complex viscoelastic properties. General practice has been to verify the analytical predictions with load factors determined from full-scale tests. The Viking mission involves an atmosphere which cannot be simulated very well on Earth. We are dependent, therefore, upon our simulation tools for Mars opening load prediction. Part of the qualification process, then, is to compare our predicted opening loads with the actual BLDT results and from this comparison make an assessment of how well we can predict opening loads on Mars.

Although it is beyond the scope of this discussion to go into the details of our opening load prediction methods, a few points can be made. The methods used represent the joint efforts of Goodyear Aerospace (GAC), NASA Langley Research Center (LRC), and Martin Marietta Corporation (MMC) and therefore consider most of the usual state-of-the-art features. Of particular concern on the Viking application are the large forebody effects on the parachute drag coefficient. Wind-tunnel data[11] shown in Fig. 8 show a dramatic difference between chute-alone drag and drag in the wake of the Viking lander. The difference has been attributed to mutual interference effects between parachute and forebody. For the purpose of opening load determination, the chute-alone data have been used on the assumption that interference drag losses take a finite length of time to be established after first inflation. The assumed value of drag coefficient used in load prediction may, of course, be reviewed to incorporate BLDT test results.

Load/elongation testing of the Dacron 52 suspension-line material has revealed some interesting properties. First, stress/strain curve nonlinearities have led us to include these effects in our simulation model rather than using a simple spring constant. Second, testing of the suspension lines at different load onset rates has revealed a strong sensitivity to this effect. The upper and lower load/elongation curves on the left in Fig. 9 were obtained for strain rates of 1.67% per second and 100% per second. It is apparent that the difference between the two

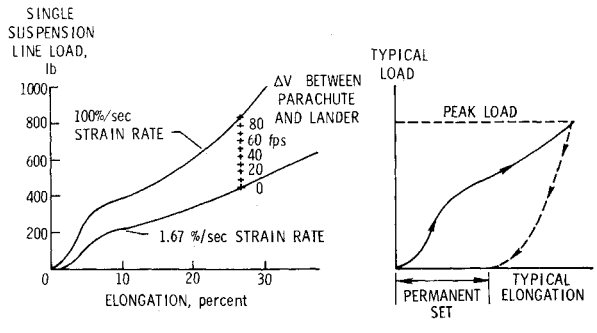

Fig. 9 Suspension-line load/elongation data.

Table 5 BLDT peak load conditions

	AV-1	AV-2	AV-3	AV-4
Mach number	1.91	1.06	0.46	1.89
Dynamic pressure, psf	11.00	4.55	7.18	8.50
Peak axial acceleration, g's	−11.2	−5.62	−7.86	−9.728
Peak load (tensiometer), lb	17393	9009	12906	16196
Peak load[a] (accelerometer), lb	18260	9408	13400	16050
Predicted load for above conditions, lb	19500	7029	12558	17123
Effective drag coefficient, F/qS	0.717	0.897	0.815	0.863
Filling time from line stretch, sec	0.56	0.64	0.81	0.56

[a] Adjusted for aeroshell drag.

curves simply reflects viscous damping and can be related to the relative velocity between lander and parachute during the inflation process. Another interesting property of textiles is the change in apparent elastic properties after peak load during the unloading cycle as noted on the right in Fig. 9. This hysteresis effect is time dependent and results in permanent deformation when the load is removed.

The parachute opening loads experienced on BLDT are recorded by tensiometers in each of the three bridle legs and by onboard accelerometers. The tensiometers are summed directly to obtain the total parachute load, whereas the accelerometer readings include aeroshell drag which must be subtracted to obtain parachute loads. The conditions at peak load are summarized in Table 5.

One must keep in mind that the opening loads recorded by the tensiometers or the accelerometers can each be in error by as much as 5%. A comparison of the actual versus predicted load data in Fig. 10 shows the in-flight measurements, however, agreeing reasonably well with each other. The predicted loads, on the other hand, seem to show a systematic error band which underpredicts at low load and overpredicts at high loads. This is a more desirable situation than the other way around and may simply reflect undue conservatism that creeps into worst-case analyses. There are several other possible explanations, however, that seem more likely. The phase relationship between load application and the natural frequency of the system may be different in reality than in the model. This is the old problem that shows up occasionally even in two tests at identical dynamic pressure because no two inflations are the same dynamically. Another explanation for the error band may lie in our assumed load/elongation and damping properties shown in Fig. 9. This is suggested by the shape of both the actual and predicted load curves in Fig. 10. Note the upper bend in the curves appears at a single line load level of 330 lb which is

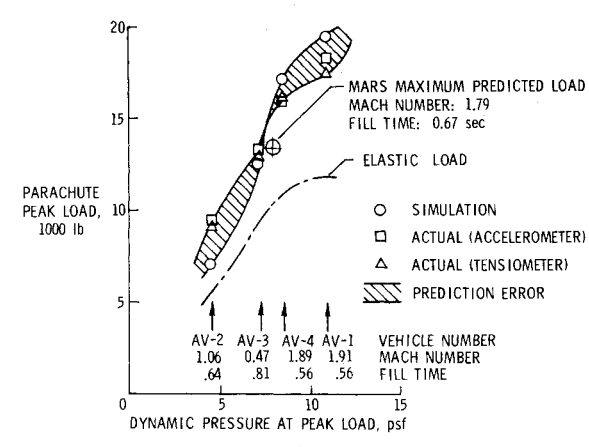

Fig. 10 Predicted vs actual load.

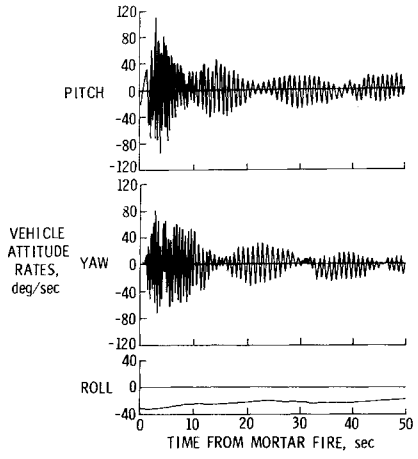

Fig. 11 Vehicle attitude rates, AV-4 flight data.

where the 100% strain-rate curve bends also. Indeed, if we plot the elastic portion of the opening load from our simulation in Fig. 10 it resembles the shape of the actual load more closely than the simulation total load which includes damping. This may imply that the shape of our assumed damping curve is in error. This last explanation seems to be the most reasonable and suggests an adjustment of our model to more nearly agree with BLDT results.

Even with no modification to our load prediction model, the BLDT results imply that we will certainly be able to predict the Mars opening load for a given set of conditions to within ± 2000 lb. At the Mars maximum predicted load level of 13,500 lb, the uncertainty in load prediction will be closer to ± 1000 lb and we will more likely overpredict than underpredict.

Load histories during parachute deployment for the BLDT flights are included in Refs. 3–6.

One of the benefits of having individual load cells at each of three bridle legs is the ability to determine the pull angle that the parachute load makes with the longitudinal axis of the vehicle. The value most significant for structural design purposes is the pull angle value occurring at peak load. This value was amazingly consistent on BLDT in spite of the wide variety of deployment conditions. The four flight values were 3.0 (AV-1), 3.0 (AV-2), 3.5 (AV-3), and 3.2 (AV-4) for an average of 3.17°.

Parachute and Vehicle Stability

One of the concerns of the decelerator qualification process is the determination of attitudes and attitude rates induced into the lander by the parachute. One object of the qualification procedure is to assess attitudes and attitude rates on BLDT and analytically extrapolate them to Mars conditions. The BLDT AV-4 attitude rates from onboard rate gyros in pitch, yaw, and roll are shown in Fig. 11. At opening shock, the peak attitude rate is 110° per second at a frequency of 2.2 cps. The peculiar beating characteristic in pitch and yaw is simply the projection on the pitch and yaw axis of a rolling vehicle of an attitude transient that is initially occurring in a specific plane. The other three BLDT flights had attitude transient response very similar in frequency, damping, and general character to that shown for AV-4. Because of the differing load and initial conditions on the other flights, however, the peak attitude rates in degrees/second were 148 (AV-1), 90 (AV-2), and 120 (AV-3).

The BLDT vehicle was aerodynamically similar to the Viking lander, but had different physical properties as indicated in Table 6.

Another difference is the fact that the Viking lander has an active attitude control system with 40 ft-lb torque and capable of controlling the vehicle at deployment to within $\pm 3°$ of aerodynamic trim in the presence of wind gusts.

Table 6 Physical property comparison

		BLDT AV-4	Viking Lander
Weight, lb		1890	1960.6
C.G. offset, Z inches		1.41	1.83
Moment of inertia, slug-ft^2	X	437/262	537/333
(before/after aeroshell	Y	335/227	285/154
separation)	Z	322/214	345/246

The Mars maximum load case (Mach 1.9 deployment) and the mean deployment have been simulated in detail. The results show the Viking maximum attitude rates to be smaller than the BLDT peak rates largely because of the lower loads, slower filling time, and effect of the attitude control system in controlling deployment conditions and providing rate damping thereafter. A review of the BLDT deployment conditions in Table 2 shows that none of the variables in the table have a good correlation with the variation in peak attitude rates. First peak load, however, shows a strong correlation with the peak rates in Fig. 12. The Mars peak rates and loads from simulation are plotted in the same figure and show a consistent trend. By adding an error band of uncertainty associated with our simulation, a peak attitude rate line for Mars extrapolated conditions is generated. If we attach a 1000-lb uncertainty to the maximum predicted Mars opening load of 13,500 lb, we observe an extrapolated peak rate of 100° per second which is in agreement with the parachute specification.

The Mars and BLDT simulations both show attitude excursions and rates less than 25° and 30° per second during steady-state descent and while experiencing wind gust conditions. A review of the film sequences taken from the recovery helicopter show BLDT attitude oscillations during descent to be within specification.

Parachute Recovery Summary

The parachute was successfully recovered on each of the BLDT flights. Detailed postflight inspection data are included in Refs. 3–6. The only significant damage occurred on AV-1 at an overtest load condition. The AV-1 parachute canopy sustained radial tears from the vent to the edge of the disk in gores 36 and 38 early in the inflation cycle.[3] Analysis of the nature of the tears and the fact that they occurred much prior to peak canopy load leads to the conclusion that the failed panels sustained frictional damage as they emerged from the deployment bag. The excessive dynamic pressure reduced the bag stripping velocity, allowing a significant amount of canopy inflation prior to bag strip. This behavior is felt to have caused the bag stripping damage. These areas were then exposed to localized high pressure during an unsymmetrical canopy inflation which caused the small initial damage to propagate into

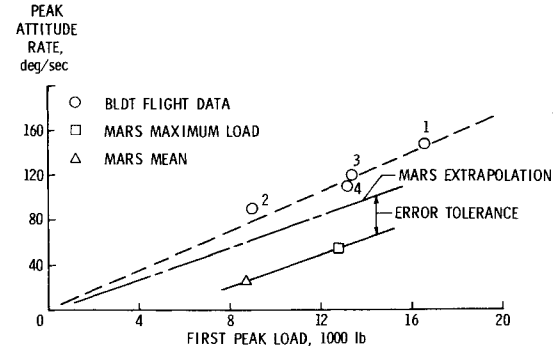

Fig. 12 Attitude rate sensitivity to load.

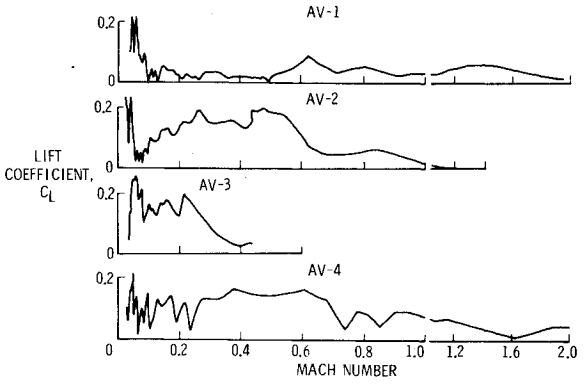

Fig. 13 Parachute lift.

large tears. In spite of the damage sustained to the canopy, the parachute maintained structural integrity and produced sufficient drag for a successful Mars mission.

Complete preflight and postflight measurements[3-6] show interesting permanent deformations in structural components. The suspension lines show the most significant permanent set which is of interest to the opening load simulation model. Between preflight measurement and postflight measurement, the parachute undergoes a heat sterilization cycle which tests have shown causes a 2% shrinkage in suspension lines. After allowing for this effect, the test results show an average 7-ft suspension-line length increase on the maximum load case (AV-1), a 3-ft average length increase on the next highest load case (AV-4) and little, if any, permanent set on the lower load cases (AV-2 and AV-3). The implication of these data is that the deformation up to some load level may be almost entirely elastic. This information may help improve our opening load prediction technique.

Parachute Drag Performance

Parachute drag performance behind a Viking lander is of utmost importance to the Viking program because of its direct effect on the amount of payload that can be landed on Mars.

Evaluation of parachute performance was conducted in several different ways. The first used onboard instrumentation to evaluate parachute forces and the second used statistical trajectory estimation methods[3-6] to produce a minimum variance match between radar position data and data obtained by integrating onboard rate gyros and accelerometers.

The onboard axial accelerometer and tensiometer data produce basically a force coefficient (C_{F_T}, C_{F_A}) along the longitudinal axis of the vehicle from the following equations:

$$C_{F_A} = A_x \cdot W_t/QS_p - C_D S_v/S_p$$

$$C_{F_T} = (F_T - A_x W_p)/QS_p$$

where:

A_x = Vehicle axial accelerometer, g's
Q = Dynamic pressure, psf
W_t = Vehicle weight, lb
W_p = Parachute weight, lb
S_p = Parachute reference area, 2206 ft^2
$C_D S_v$ = Vehicle drag area, 108 ft^2
F_t = Summation of tensiometer, lb

Plots of the above force coefficients[3-6] are highly oscillatory, reflecting the natural elastic frequency of the two-body spring mass system and noise on both the accelerometer and tensiometer data. When steady-state descent conditions are achieved, the data become practically useless because noise obscures variation in the parameter of interest. These shortcomings led to a search for a better method of extracting parachute drag performance.

Efforts to match radar trajectory data with reconstructed trajectories suggested the likelihood of parachute lift acting normal to the velocity vector. If we assume the mismatch is due to parachute lift and not gross errors in our wind estimates, the rather consistent lifting behavior shown in Fig. 13 is established. The lift coefficient is seen to generally increase as Mach number decreases and seems to have the lowest average magnitude on AV-1 which had the damaged canopy. The radar tracking data reveal that the lift vector rotates rather unsystematically around the velocity vector at varying rates and directions and sometimes stops altogether.

Parachute drag performance is obtained from the lift-producing reconstructed trajectories using the following equation:

$$C_{D_P} = M_T(\Delta V - g\sin\gamma)/qS_p - C_D S_v/S_p$$

where:

M_T = Total system mass, slugs
ΔV = Change in relative velocity between two time points, fps^2
g = Gravitational acceleration, 32.2 fps^2
γ = Flight-path angle, average value between time points
q = Average dynamic pressure between time points

The use of ΔV in the above equation instead of the onboard axial accelerometer results in defining a drag coefficient rather than a force coefficient and filters the data very effectively. The drag-coefficient curves for the four BLDT flights are shown to fall within the required envelope in Fig. 14 with a few minor exceptions. The drag performance at supersonic conditions is higher than anticipated (solid line) and appears to average slightly lower than predicted subsonically. There is evidence of drag degradation in the transonic region as indicated by wind-tunnel results. The oscillatory nature of the drag coefficients in the transonic region is concluded to result from canopy motion in and out of the wake of the forebody. The characteristic dip in drag coefficient at aeroshell separation has little influence on successful separation.

Conclusions

The following major conclusions support the decelerator qualification objectives of the Viking program.

a) The mortar provides sufficient velocity and margin to support full deployment of the parachute.

b) Parachute ejection from mortar fire through line stretch, bag strip, and initial inflation is free of significant anomalies.

c) The parachute maintains a very stable drag shape after a short period of initial inflation area oscillations.

d) Sufficient drag performance is produced to support Viking mission requirements and to achieve satisfactory aeroshell

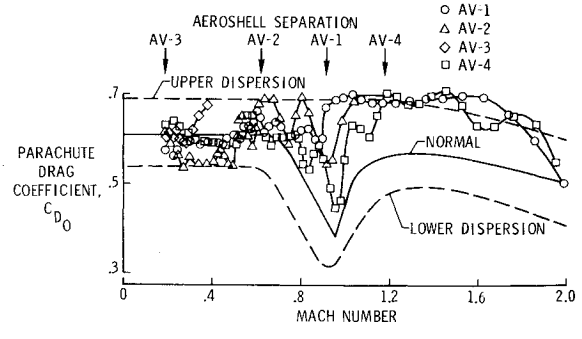

Fig. 14 Parachute drag coefficient compared with steady-state envelope.

separation. The drag coefficient produced by the parachute in the presence of the Viking forebody falls within the required envelope of Fig. 14 with few minor deviations of no significance. There is evidence of drag degradation in the wake of the entry vehicle at transonic velocity as was expected.

e) Lander oscillations in quasi-steady-state descent with no wind will be less than $\pm 25°$ on Mars. Attitude rates during terminal descent on Mars will be less than 30° per sec. The maximum attitude rate at parachute opening shock will be approximately 100° per sec.

f) Parachute structural integrity has been proven supersonically at load conditions approximately 30% greater than Mars Peak load conditions. Additionally, subsonic development and qualifications bomb drop tests have proven the structure at stress levels equivalent to 1.5 times the Mars design values.

The results of the BLDT program and low-altitude development and qualification bomb drop tests show that the performance objectives of the Viking decelerator qualification program have been successfully met.

References

[1] Reichenau, D. E. A., "Aerodynamic Characteristics of Disk-Gap-Band Parachutes in the Wake of Viking Entry Forebodies at Mach Numbers from 0·2 to 2·6," AEDC-TR-72-78, July 1972, Arnold Engineering Development Center, Tullahoma, Tenn.

[2] Murrow, H. N., Eckstrom, C. V., and Henke, D., "Development Flight Tests of the Viking Decelerator System," AIAA Paper 73-455, Palm Springs, Calif., 1973.

[3] Hicks, F., et al., "Balloon Launched Decelerator Test Program Post-Flight Test Report BLDT Vehicle AV-1," CR-112176, Sep. 1972, NASA.

[4] Hicks, F., et al., "Balloon Launched Decelerator Test Program Post-Flight Test Report BLDT Vehicle AV-2," CR-112177, Dec. 1972, NASA.

[5] Hicks, F., et al., "Balloon Launched Decelerator Test Program Post-Flight Test Report BLDT Vehicle AV-3," CR-112178, Jan. 1973, NASA.

[6] Hicks, F., et al., "Balloon Launched Decelerator Test Program Post-Flight Test Report BLDT Vehicle AV-4," CR-112179, Oct. 1972, NASA.

[7] Brecht, J., Mehring, R., and Pleasants, J., "The Viking Mortar: Design, Development, and Flight Qualification," AIAA Paper 73-458, Palm Springs, Calif., 1973.

[8] Pleasants, J. E., "Parachute Mortar Design," AIAA Paper 73-459, Palm Springs, Calif., 1973.

[9] Darnell, W. L., Henning, A. B., and Lundstrom, R. R., "Flight Test of a 15-Foot (4.6 Meter) Diameter 120° Conical Spacecraft Simulating Parachute Deployment in a Mars Atmosphere," TN D-4266, 1967, NASA.

[10] Raper, J. L., Michel, F. C., and Lundstrom, R. R., "The Viking Parachute Qualification Test Technique," AIAA Paper 73-457, Palm Springs, Calif., 1973.

[11] Steinberg, S., Siemers, P. M., III, and Slayman, R. G., "Development of the Viking Parachute Configuration by Wind-Tunnel Investigation," AIAA Paper 73-454, Palm Springs, Calif., 1973.

[12] Whitlock, C. H. and Bendura, R. J., "Inflation and Performance of Three Parachute Configurations From Supersonic Flight Tests in a Low-Density Environment," TN D-5296, July 1969, NASA.

[13] "Performance of and Design Criteria for Deployable Aerodynamic Decelerators," ASD-TR-61-579, U.S. Air Force, Dec. 1963.

[14] Heinrich, H. G. and Noreen, R. A., "Analysis of Parachute Opening Dynamics With Supporting Wind Tunnel Experiments," AIAA Paper 68-924, El Centro, Calif., 1968.

[15] Berndt, R. J. and DeWeese, J. H., "The Opening Force of Solid Cloth, Personnel Type Parachutes," AIAA Paper 70-1167, Dayton, Ohio, 1970.

[16] Toni, R. A., "Theory on the Dynamics of a Parachute System Undergoing Its Inflation Process," AIAA Paper 70-1170, Dayton, Ohio, 1970.